

Predictors of angle widening after laser iridotomy in Chinese patients with primary angle-closure suspect using ultrasound biomicroscopy

Xue-Ting Pei, Shu-Hua Wang, Xia Sun, Hong Chen, Bing-Song Wang, Shu-Ning Li, Tao Wang

Beijing Tongren Eye Center, Beijing Tongren Hospital, Capital Medical University, Beijing Ophthalmology and Visual Science Key Laboratory, Beijing 100730, China

Correspondence to: Tao Wang. Beijing Tongren Eye Center, Beijing Tongren Hospital, Capital Medical University, Beijing Ophthalmology and Visual Science Key Laboratory, Dongjiaominxiang No.1, Dongcheng District, Beijing 100730, China. stevenwa@sohu.com

Received: 2021-02-17 Accepted: 2021-09-23

Abstract

● **AIM:** To assess the predictive value of baseline parameters of ultrasound biomicroscopy (UBM) for angle widening after prophylactic laser peripheral iridotomy (LPI) in patients with primary angle-closure suspect (PACS).

● **METHODS:** Angle-opening distance (AOD), trabecular iris angle (TIA), iris thickness, trabecular-ciliary process angle, and trabecular-ciliary process distance were measured using UBM performed before and two weeks after LPI. Iris convexity (IC), iris insertion, angulation, and ciliary body (CB) size and position were graded. Uni- and multivariate regression analyses were used to determine factors predicting the change in AOD (Δ AOD500, calculated as an angle width change before and after LPI) in all quadrants and in subgroup quadrants based on IC.

● **RESULTS:** In 94 eyes of 94 patients with PACS, LPI led to angle widening with increases in AOD500 and TIA ($P < 0.01$). Multivariable regression analysis showed that IC ($P < 0.001$), CB position ($P = 0.007$) and iris insertion ($P = 0.049$) were significantly predictive for Δ AOD500. All quadrants were categorized into extreme IC (27.8%), moderate IC (62.3%), and absent IC (9.9%) subgroups. The AOD500 increased by 220% and no other predictive factor was found in the extreme IC quadrants. The AOD500 increased by 55%, and baseline iris angulation was predictive for smaller changes in Δ AOD500 in the moderate IC quadrants.

● **CONCLUSION:** In PACS patients, quadrants with greater iris bowing predict substantial angle widening after LPI. Quadrants with a flatter iris, anteriorly positioned CB, and

basal iris insertion are associated with less angle widening after LPI. Quadrants with iris angulation as well as a flatter iris configuration predict a smaller angle change after LPI.

● **KEYWORDS:** laser peripheral iridotomy; angle opening distance; ultrasound biomicroscopy; iris convexity; iris angulation

DOI:10.18240/ijo.2022.02.07

Citation: Pei XT, Wang SH, Sun X, Chen H, Wang BS, Li SN, Wang T. Predictors of angle widening after laser iridotomy in Chinese patients with primary angle-closure suspect using ultrasound biomicroscopy. *Int J Ophthalmol* 2022;15(2):233-241

INTRODUCTION

Primary angle-closure glaucoma (PACG) is a main cause of bilateral irreversible blindness worldwide. Approximately 23.36 million people aged 40-80y had PACG worldwide in 2020, and the number of the case is estimated to reach 32.04 million in 2040^[1]. Asian patients account for approximately 77% of worldwide angle-closure glaucoma cases^[1-2]. Angle-closure glaucoma includes three categories: primary angle-closure suspect (PACS) with narrow angles that are predisposed to angle closure, primary angle-closure (PAC) with occluded angle and trabecular obstruction without glaucomatous optic disc damage, and PACG with glaucomatous optic neuropathy^[3-4]. The commonly known pathological mechanism for angle-closure glaucoma is pupillary block (PB), which prevents aqueous flow and thus results in anterior bowing of the peripheral iris^[5]. Laser peripheral iridotomy (LPI) has long been the first-line standard intervention for angle closure based on the elimination of PB, and can be used for treating symptomatic cases and as prophylactic treatment in PACS patients^[6]. However, PACS patients appear to gain less benefit from prophylactic LPI for two reasons. First, the conversion rate from PACS to angle-closure disease is very low^[7]. Second, after LPI, persistent angle closure still exists in many eyes^[8-10], which develop peripheral anterior synechia^[11]. Under this condition, non-PB mechanisms as well as the PB mechanism often simultaneously contribute

to angle closure, including thick peripheral iris, anteriorly positioned ciliary body (CB), and plateau iris^[6,12-14]. Thus, the use of LPI as prophylactic treatment for narrow angle is being considered^[15].

Anterior segment optical coherence tomography (AS-OCT) parameters are commonly used to assess predictive parameters for enlargement of the anterior chamber angle following LPI. It has been reported that increased postoperative angle widening is correlated with a shorter baseline angle-opening distance (AOD) and axial length as well as a greater baseline anterior chamber depth (ACD), iris curvature, and lens vault^[16-17]. These parameters mainly reflect factors associated with PB. However, AS-OCT imaging has some disadvantages such as limited resolution and difficulty in identifying the location of the ciliary processes and iris angulation. In addition, images of only nasal and temporal quadrants are obtained by AS-OCT, and thus, the analysis of superior and inferior quadrants is not possible.

The noninvasive ultrasound biomicroscopy (UBM) can be used to view structures behind the iris^[18]. A cross-sectional view of the anterior chamber angle anatomy and the relative position of the iris and CB can be achieved by radially oriented scanning through the limbus. UBM can provide insight into the underlying mechanism of PAC diseases and aid the identification of risk factors for a progressive narrow angle after LPI. In the present study, UBM images of four quadrants were used to quantitatively measure and qualitatively describe the anterior segment morphology in PACS patients before and after LPI. The morphological parameters were analyzed to study the possible predictive factors for angle widening as the LPI outcome. Moreover, we categorized all quadrants according to the configuration of iris convexity (IC) to analyze the effect of LPI and investigated the predictive factors for each subgroup.

SUBJECTS AND METHODS

Ethical Approval The study was approved by the Ethics Committee Board of Beijing Tongren Hospital and conducted in accordance with the tenets of the Declaration of Helsinki. All patients provided written informed consent ahead of participation.

Patients This retrospective study was performed at the Eye Center of Beijing Tongren Hospital. The medical records of consecutive patients who visited the glaucoma clinic between January 2019 and September 2020 were reviewed. The inclusion criteria were as follows: 1) age >50y; 2) PACS diagnosis and UBM examination; 3) treatment with LPI. Patients were excluded if they had secondary angle closure, previous attack of acute angle closure, cataract (visual acuity, worse than 20/40), a history of any eye injuries (intraocular surgery or penetrating eye injury), or used topical or systemic

medications that could affect the anterior chamber angle. All participants underwent complete ophthalmic examinations, including a review of their medical history, measurement of best corrected visual acuity, slit-lamp biomicroscopy, intraocular pressure measurements with Goldmann applanation tonometry, gonioscopy, funduscopy examination with a 90-diopter lens, stereoscopic optic disc photography, visual field test, and UBM. The visual field test was analyzed using a Humphrey Visual Field Analyzer II (Carl Zeiss Meditec, Dublin, California, USA) with the standard Swedish interactive threshold algorithm in a 24-2 test pattern.

PACS was defined as follows: 1) having 180° of the posterior trabecular meshwork, which was not visualized on the basis of static gonioscopic examination; 2) intraocular pressure <21 mm Hg; 3) no peripheral anterior synechiae (abnormal adhesions of the iris to the angle by more than half a clock hour in width); 4) glaucomatous optic neuropathy [a vertical cup-to-disc (C/D) ratio > 0.7, C/D asymmetry > 0.2, focal notching, or visual field changes compatible with glaucoma]. Only one eye was chosen randomly in patients with two eligible eyes and included in the analysis.

Gonioscopy Slit lamp gonioscopy was performed using a Goldmann-type, one-mirror lens (Ocular OSMG, Bellevue WA, USA). Gonioscopic examinations were conducted by an experienced observer (Pei XT). Indentation gonioscopy was used to identify the cause of angle closure (apposition or peripheral anterior synechiae). Appositional angle closure was verified by gonioscopy for all patients.

Laser Peripheral Iridotomy LPI was performed after topical application of 2% pilocarpine for pupil constriction (Zhenrui; Bausch and Lomb Freda, Shandong, China) and proparacaine (0.5%) for anesthesia (Alcaine; Alcon, Fort Worth, TX, USA). A neodymium-yttrium-aluminum-garnet laser was set at variable energy levels between 6 and 8 mJ (1-10 shots). One opening was created using an Abraham lens, and a crypt was selected in the peripheral iris when possible. UBM was used to confirm iridotomies. Prednisolone eye drops (4 times daily for 3d) was applied following the intervention.

All cases were examined with UBM before and 2wk after LPI. UBM examinations were performed with a UBM Model MD-300L instrument (MEDA Co., Ltd., Tianjin, China). After topical application of proparacaine (0.5%) in both eyes, an eyecup filled with sterile normal saline was used as a coupling agent. Images were taken under the same lighting conditions (3.25 cd/m²) by the same experienced operator. Under a sufficient lighting condition, eyes were examined in axial section, and the probe was kept perpendicular to the corneal-scleral surface. Images were obtained from the superior, nasal, inferior and temporal quadrants as well as the center of the pupil.

Image Analysis Image J 1.51 software (Wayne Rasband, NIH, Rockville, MD, USA) was used for analyzing all images (Figure 1). The scleral spur (SS) was located based on the difference in the tissue density between the collagen fibers of the SS and the longitudinal muscle of the CB.

The following quantitative anterior segment parameters were measured (Figure 1). Pupil diameter was defined as the distance between pupillary margins. ACD was measured by the distance between the corneal endothelium and the anterior surface of the lens. AOD500 was calculated as the distance from the corneal endothelium to the anterior iris perpendicular to a line drawn along the trabecular meshwork at 500 μm from the SS. Trabecular iris angle (TIA) was measured with the SS as the apex and the corneal endothelium and superior surface of the iris as the arms of the angle. IT750 was defined as the thickness of the iris thickness 750 μm from the SS. Trabecular-ciliary process angle (TCA) was measured with the SS as the apex and the corneal endothelium and superior surface of the ciliary process as the arms of the angle. Trabecular-ciliary process distance (TCPD) was measured as the perpendicular length of the line extending from the corneal endothelium 500 μm from the SS through the posterior surface of iris to the ciliary process.

The following qualitative parameters were assessed according to standard UBM photographs (Figure 2). IC (absent/moderate/extreme) was graded by the curvature of the posterior surface of the iris. Iris insertion (basal/middle/apical) was graded based on the location of the iris insertion into the CB. Iris angulation (none/mild/pronounced) was identified based on the change of the iris at the insertion point into the CB. CB size was defined as the greatest distance between the apex of the CB and base, in reference to the limbal cornea thickness (small, less than limbal cornea thickness; medium, greater than the limbal cornea thickness by <2 -fold; and large, greater than the limbal cornea thicknesses by ≥ 2 -fold). CB position was categorized as neutral or anteriorly positioned on the basis of the direction of the axis of the CB processes.

Fifteen eyes (60 quadrants) were randomly selected for assessment of intra-examiner reproducibility. The quantitative parameters were measured repeatedly by the same observer. Qualitative parameters were assessed independently by two glaucoma specialists (Pei XT and Sun X). If the specialists had different opinions, a third experienced examiner (Wang SH) made the final decision.

Statistical Analysis Statistical analyses were performed using SPSS version 20.0 (SPSS Inc., Chicago, Illinois, USA). Intra-examiner repeatability for UBM parameters was assessed by intraclass correlation coefficients. The paired Student's *t*-test was performed to analyze the differences in the parameters before and after LPI. Covariance was used for subgroup differences in the parameters with pupil diameter as a

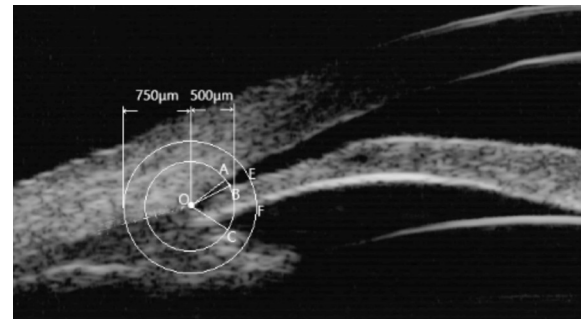


Figure 1 Quantitative parameters measured on ultrasound biomicroscopic images A circle with 500 μm in radius was drawn using the SS (O) as the center. The points of intersection were at the back of the cornea (A) and the anterior surface of the CB (C). The AOD was measured on a line perpendicular to the plane of the trabecular surface 500 μm anterior to the SS and extended to meet the surface of the iris (B); the TCPD was a line measured between A and C. For iris thickness, a circle with 750 μm in radius was drawn using the SS (O) as the center, and the iris thickness was the distance from the intersection point (E) on the anterior surface of the iris to the intersection point (F) on the posterior surface. The TIA was the angle AOB; the TCA was the angle AOC.

covariate. The Chi-square test was used to compare categorical variables of qualitative assessment.

Linear regression adjusted for PD was performed to assess the association between baseline UBM parameters and changes in AOD500 (ΔAOD500) defined as the difference between AOD500 after LPI and AOD500 before LPI. Predictors of angle widening was determined by using multivariable forward stepwise linear regression algorithms. Variables with a probability value ≤ 0.10 on univariate analysis were included in the multivariate analysis. *P* values < 0.05 were considered statistically significant.

RESULTS

A total of 94 eyes of 94 Chinese patients with PACS (65 females and 29 males) were included in the study. The mean patient age was $61.5 \pm 7.8\text{y}$ (range, 50-72y). The intra-examiner intraclass coefficient values for the UBM parameters were between 0.875 and 0.927.

The mean pupil diameter was 3.3 ± 0.7 mm before LPI and 3.2 ± 0.8 mm after LPI ($P=0.312$). The mean ACD was 2.10 ± 0.43 mm before LPI and 2.11 ± 0.39 mm after LPI ($P=0.165$). The pupil diameter and ACD before and after LPI were not significantly different.

Table 1 summarizes the UBM parameters in the four quadrants before and after LPI. There were significant differences in angle width in the four quadrants before and after LPI. The parameters for the anterior chamber angle width increased significantly after LPI. For all quadrants, the mean AOD500 increased by 100% from 0.10 ± 0.07 mm before LPI to 0.20 ± 0.10 mm after LPI ($P < 0.01$). The mean TIA increased

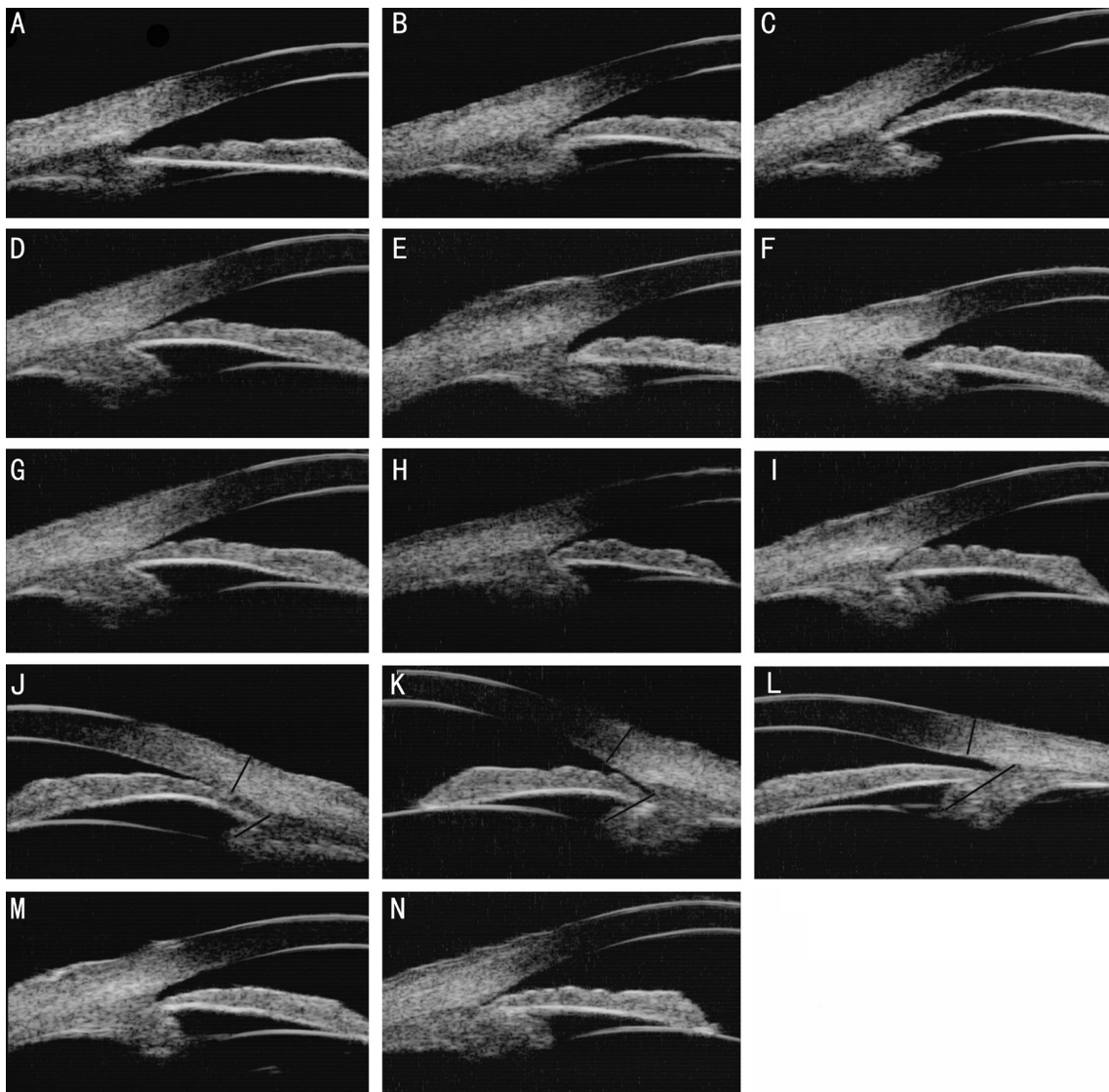


Figure 2 Standard photographs were used to assess UBM results A: Absent IC; B: Moderate IC; C: Extreme IC. D: Basal iris insertion; E: Middle iris insertion; F: Apical iris insertion; G: No iris angulation; H: Mild iris angulation; I: Pronounced iris angulation; J: Small CB; K: Medium CB; L: Large CB; M: Neutral CB position; N: Anterior CB position.

significantly from $9^{\circ}\pm 7^{\circ}$ before LPI to $19^{\circ}\pm 10^{\circ}$ after LPI ($P<0.01$). However, the angle width decreased or remain unchanged in 37.4% of quadrants.

Linear regression analyses showed that greater IC and shorter IT750 predicted greater angle widening following LPI, which was defined as an increase in AOD500 after LPI ($\Delta\text{AOD500}>0$) in each quadrant ($P<0.05$). Multivariable stepwise regression analysis (overall model adjusted $R^2=0.64$; $P<0.001$) demonstrated that IC and CB position were predictive for angle changes after LPI. Iris insertion reached marginal significance as a predictor for angle widening. Greater angle widening following LPI was correlated with a greater IC at baseline ($P<0.001$). A more anteriorly positioned CB ($P=0.007$) and a closer basal iris insertion ($P=0.049$) were associated with smaller angle widening after LPI (Table 2). Linear regression analyses adjusted for sex and intraocular pressure as covariates were further performed, and the

results were similar to the analysis without adjusted sex and intraocular pressure as covariates.

All quadrants were subcategorized according to IC, as the extreme IC group (104 quadrants, 27.8%), moderate IC group (235 quadrants, 62.3%), and absent IC group (37 quadrants, 9.9%). Table 3 summarizes the UBM parameters in the three groups before and after LPI. Angle widening was significantly different among the groups. Compared with pre-LPI values, the AOD500 was increased significantly by 220% after LPI in the extreme IC quadrants and increased significantly by 55% in the moderate IC quadrants. No statistically significant difference in AOD500 before and after LPI was noted in the absent IC group. The TCA in the moderate IC group was significantly narrower than that in the extreme IC group.

Linear regression analyses and multivariable stepwise regression analysis were performed in each subgroup. Univariate linear regression analysis showed that no anatomic

Table 1 Quantitative measurement and qualitative grading of UBM images in four quadrants before and after LPI

| Parameters | Quadrant | | | |
|---|-----------|-----------|-----------|-----------|
| | Superior | Nasal | Inferior | Temporal |
| AOD500 (mm) | | | | |
| Pre-LPI | 0.03±0.04 | 0.13±0.07 | 0.09±0.06 | 0.14±0.06 |
| Post-LPI | 0.16±0.08 | 0.23±0.09 | 0.20±0.11 | 0.26±0.13 |
| <i>P</i> | <0.001 | <0.001 | <0.001 | <0.001 |
| TIA (degrees) | | | | |
| Pre-LPI | 4.0±3.8 | 10.3±4.9 | 9.0±6.2 | 11.4±8.3 |
| Post-LPI | 15.0±8.3 | 18.7±10.9 | 17.0±9.3 | 20.0±11.8 |
| <i>P</i> | 0.005 | 0.019 | 0.003 | 0.018 |
| IT750 (mm) | | | | |
| Pre-LPI | 0.31±0.06 | 0.36±0.05 | 0.35±0.04 | 0.35±0.06 |
| Post-LPI | 0.35±0.05 | 0.38±0.06 | 0.39±0.05 | 0.33±0.04 |
| <i>P</i> | 0.036 | 0.142 | 0.025 | 0.376 |
| TCA (degrees) | | | | |
| Pre-LPI | 40.4±11.1 | 57.3±11.8 | 55.3±14.1 | 61.4±17.5 |
| Post-LPI | 53.0±15.4 | 57.0±10.9 | 59.7±23.2 | 57.3±12.1 |
| <i>P</i> | 0.078 | 0.938 | 0.620 | 0.284 |
| TCPD500 (mm) | | | | |
| Pre-LPI | 0.43±0.10 | 0.59±0.10 | 0.57±0.13 | 0.62±0.17 |
| Post-LPI | 0.53±0.13 | 0.58±0.08 | 0.58±0.15 | 0.59±0.11 |
| <i>P</i> | 0.121 | 0.525 | 0.888 | 0.262 |
| Iris convexity (absent/moderate/extreme) | | | | |
| Pre-LPI | 6/58/30 | 10/58/26 | 8/51/35 | 13/66/15 |
| Post-LPI | 94/0/0 | 94/0/0 | 94/0/0 | 94/0/0 |
| Iris angulation (none/mild/pronounced) | | | | |
| Pre-LPI | 74/16/4 | 67/20/7 | 66/23/5 | 54/28/12 |
| Post-LPI | 81/13/0 | 72/15/7 | 73/16/5 | 57/27/10 |
| <i>P</i> | 0.081 | 0.309 | 0.514 | 0.282 |
| Iris insertion (basal/middle/apical) | | | | |
| Pre-LPI | 60/31/3 | 47/44/3 | 56/36/2 | 36/52/6 |
| CB relative size (small/medium/large) | | | | |
| Pre-LPI | 35/39/20 | 28/50/16 | 28/45/21 | 12/46/36 |
| CB position (neutral/anterior) | | | | |
| Pre-LPI | 37/57 | 25/69 | 45/49 | 40/54 |

AOD500: Angle-opening distance at 500 µm from scleral spur; LPI: Laser peripheral iridotomy; TIA: Trabecular iris angle; IT750: Iris thickness at 750 µm from scleral spur; TCA: Trabecular-ciliary process angle; TCPD500: Trabecular-ciliary process distance at 500 µm from scleral spur; CB: Ciliary body.

factors were significantly associated with ΔAOD500 in the extreme IC group (Table 4). Iris angulation was found to be a predictor for ΔAOD500 in the moderate IC group (*P*=0.029). A greater iris angulation before LPI was associated with a smaller change in the angle width following LPI (Table 5). Linear regression analyses adjusted for sex and intraocular pressure as covariates were further performed, and the results were similar to the analysis without adjusted sex and intraocular pressure as covariates.

DISCUSSION

The present study found that prophylactic LPI treatment

increased the anterior chamber angle width in Chinese patients with PACS. We assessed the potential predictive parameters for the change in the angle measured by UBM. The angle widening observed in each quadrant was associated with three baseline factors: IC, CB position, and iris insertion. As IC was the key factor that affected the effect of LPI, we categorized all quadrants according to the IC grading. Extreme IC quadrants were associated with the best outcomes from LPI, and no baseline parameters were significantly associated with angle widening. LPI reduced angle width in moderate IC quadrants compared with extreme quadrants, and the angle width change

Table 2 Uni- and multivariate linear regression analyses of the association between baseline UBM parameters and ΔAOD500 after LPI in all quadrants

| Parameters | SE | Univariate B coefficient (95%CI) | <i>P</i> | SE | Multivariate B coefficient (95%CI) | <i>P</i> |
|-----------------|-------|----------------------------------|----------|-------|------------------------------------|----------|
| PreAOD500 | 0.541 | -0.653 (-1.778, 0.473) | 0.241 | | | |
| PreTIA | 0.006 | 0.004 (-0.007, 0.016) | 0.787 | | | |
| PreIT750 | 0.354 | 0.037 (-0.700, 0.774) | 0.010 | | | |
| PreTCA | 0.004 | -0.001 (-0.008, 0.007) | 0.849 | | | |
| PreTCPD | 0.395 | 0.242 (-0.580, 1.064) | 0.547 | | | |
| Iris convexity | 0.044 | 0.103 (0.012, 0.193) | 0.000 | 0.023 | 0.125 (0.077, 0.173) | 0.000 |
| Iris angulation | 0.045 | -0.056 (-0.149, 0.037) | 0.227 | | | |
| Iris insertion | 0.039 | 0.065 (-0.001, 0.132) | 0.053 | 0.028 | 0.058 (0.000, 0.117) | 0.049 |
| CB position | 0.018 | -0.061 (-0.153, 0.033) | 0.002 | 0.041 | -0.121 (-0.206, -0.036) | 0.007 |
| CB size | 0.022 | -0.014 (-0.061, 0.033) | 0.537 | | | |

SE: Spherical equivalent; AOD500: Angle-opening distance at 500 μm from scleral spur; TIA: Trabecular iris angle; IT750: Iris thickness at 750 μm from scleral spur; TCA: Trabecular-ciliary process angle; TCPD500: Trabecular-ciliary process distance at 500 μm from scleral spur; CB: Ciliary body.

Table 3 Comparison of quantitative measurements and qualitative grading of UBM parameters before and after LPI in three iris convexity grading subgroups

| Parameters | Subgroups | | | <i>P</i> (intergroup) |
|--|-----------------------------|------------------------------|---------------------------|-----------------------|
| | Extreme IC (<i>n</i> =104) | Moderate IC (<i>n</i> =235) | Absent IC (<i>n</i> =37) | |
| AOD500 (mm) | | | | |
| Pre-LPI | 0.10±0.08 | 0.09±0.06 | 0.16±0.13 | 0.305 |
| Post-LPI | 0.32±0.11 | 0.14±0.09 | 0.20±0.12 | 0.003 |
| <i>P</i> | <0.001 | 0.005 | 0.552 | |
| TIA (degrees) | | | | |
| Pre-LPI | 9.1±6.6 | 8.4±6.3 | 15.6±10.5 | 0.220 |
| Post-LPI | 29.8±11.2 | 12.3±7.1 | 18.6±11.8 | <0.001 |
| <i>P</i> | <0.001 | 0.008 | 0.707 | |
| IT750 (mm) | | | | |
| Pre-LPI | 0.30±0.04 | 0.36±0.05 | 0.41±0.04 | 0.004 |
| Post-LPI | 0.33±0.06 | 0.38±0.04 | 0.40±0.05 | 0.038 |
| <i>P</i> | 0.057 | 0.037 | 0.392 | |
| TCA (degrees) | | | | |
| Pre-LPI | 60.5±17.2 | 46.8±12.1 | 64.6±16.0 | 0.032 |
| Post-LPI | 70.5±11.8 | 48.7±11.4 | 61.3±13.3 | <0.001 |
| <i>P</i> | 0.046 | 0.447 | 0.233 | |
| TCPD500 (mm) | | | | |
| Pre-LPI | 0.61±0.17 | 0.49±0.10 | 0.65±0.14 | 0.055 |
| Post-LPI | 0.66±0.09 | 0.50±0.12 | 0.60±0.11 | <0.001 |
| <i>P</i> | 0.448 | 0.758 | 0.162 | |
| Iris angulation (none/mild/pronounced) | | | | |
| Pre-LPI | 78/26/0 | 168/51/16 | 15/9/13 | <0.001 |
| Post-LPI | 91/13/0 | 177/46/12 | 15/12/10 | <0.001 |
| <i>P</i> | 0.085 | 0.680 | 0.764 | |
| Iris insertion (basal/middle/apical) | | | | |
| Pre-LPI | 70/34/0 | 122/104/9 | 9/24/4 | <0.001 |
| CB relative size (small/medium/large) | | | | |
| Pre-LPI | 39/51/14 | 64/105/66 | 0/24/13 | 0.003 |
| CB position (neutral/anterior) | | | | |
| Pre-LPI | 49/55 | 84/150 | 15/22 | 0.278 |

IC: Iris convexity; AOD500: Angle-opening distance at 500 μm from scleral spur; LPI: Laser peripheral iridotomy; TIA: Trabecular iris angle; IT750: Iris thickness at 750 μm from scleral spur; TCA: Trabecular-ciliary process angle; TCPD500: Trabecular-ciliary process distance at 500 μm from scleral spur; CB: Ciliary body.

Table 4 Uni- and multivariate linear regression analyses of the associations between baseline UBM parameters and ΔAOD500 after LPI in the extreme IC quadrants

| Parameters | SE | Univariate B coefficient (95%CI) | P |
|-----------------|-------|----------------------------------|-------|
| PreAOD500 | 2.055 | 0.184 (0.095, 0.273) | 0.943 |
| PreTIA | 0.024 | -0.026 (-0.049, -0.003) | 0.616 |
| PreIT750 | 3.438 | -1.844 (-2.645, -1.032) | 0.687 |
| PreTCA | 0.032 | -0.037 (-0.097, 0.068) | 0.453 |
| PreTCPD | 4.849 | 7.958 (3.469, 11.395) | 0.348 |
| Iris angulation | 0.301 | -0.557 (-0.976, -0.203) | 0.315 |
| Iris insertion | 0.264 | 0.220 (0.002, 0.462) | 0.558 |
| CB position | 0.821 | 0.578 (0.390, 0.836) | 0.609 |
| CB Size | 0.212 | -0.074 (-0.134, 0.037) | 0.787 |

SE: Spherical equivalent; AOD500: Angle-opening distance at 500 μm from scleral spur; TIA: Trabecular iris angle; IT750: Iris thickness at 750 μm from scleral spur; TCA: Trabecular-ciliary process angle; TCPD500: Trabecular-ciliary process distance at 500 μm from scleral spur; CB: Ciliary body.

Table 5 Uni- and multivariate linear regression analyses of the associations between baseline UBM parameters and ΔAOD500 after LPI in moderate IC quadrants

| Parameters | SE | Univariate B coefficient (95%CI) | P | SE | Multivariate B coefficient (95%) | P |
|-----------------|-------|----------------------------------|-------|-------|----------------------------------|-------|
| PreAOD500 | 0.492 | -0.411 (-1.524, 0.702) | 0.425 | | | |
| PreTIA | 0.005 | 0.004 (0.008, 0.015) | 0.499 | | | |
| PreIT750 | 0.272 | 0.392 (-0.224, 1.008) | 0.184 | | | |
| PreTCA | 0.003 | 0.002 (-0.004, 0.008) | 0.396 | | | |
| PreTCPD | 0.289 | -0.288 (-0.942, 0.367) | 0.346 | | | |
| Iris angulation | 0.033 | -0.080 (-0.157, -0.009) | 0.029 | 0.033 | -0.080 (-0.150, -0.009) | 0.029 |
| Iris insertion | 0.033 | 0.046 (-0.029, 0.120) | 0.198 | | | |
| CB position | 0.035 | -0.059 (-0.138, 0.020) | 0.124 | | | |
| CB size | 0.019 | 0.018 (-0.026, 0.062) | 0.378 | | | |

SE: Spherical equivalent; AOD500: Angle-opening distance at 500 μm from scleral spur; TIA: Trabecular iris angle; IT750: Iris thickness at 750 μm from scleral spur; TCA: Trabecular-ciliary process angle; TCPD500: Trabecular-ciliary process distance at 500 μm from scleral spur; CB: Ciliary body.

was significantly associated with baseline iris angulation. The angle width remained unchanged in the absent IC quadrants. Our results are consistent with previous research showing that the peripheral anterior chamber width increases following LPI^[16,19-22]. Our data showed LPI led to an immediate increase in the anterior chamber angle width in Chinese PACS patients. The mean AOD500 increased significantly by 100% (from 0.10 mm before LPI to 0.20 mm after LPI). In previous studies of eyes without PAS, the quantitative angle-width parameters increased after LPI, and the mean width changes varied from 54.7% to 135% based on the UBM or AS-OCT results^[16,19]. However, in the present study, the AOD500 remained unchanged or decreased in one-third of all quadrants after LPI. He *et al*^[22] found that after LPI, about 60% of the eyes in Chinese PACS patients still had appositional closure detected by UBM. Meduri *et al*^[16] reported that approximately 70% of angles opened in more than two quadrants, whereas 50% opened in all four quadrants after LPI in patients with PAC and

PACG, especially in South Indian patients with PACS. The outcomes of LPI differed in distinct anatomical quadrants. Our results showed that IC is the key predictive determinant associated with the outcome of LPI, which is used to remove the PB. The increase in angle width after LPI was associated with the degree of IC at baseline, suggesting that the greater preoperative PB would be associated with larger peripheral anterior chamber angle width after LPI. Therefore, IC can reflect the severity of PB, and iris bowing predicts the degree of relative PB. Consistent with our findings, previous studies reported that LPI-induced angle widening is correlated with less iris curvature measured by AS-OCT^[16-17,20,23] and greater baseline IC^[17,23]. Multiple pathogenic mechanisms contribute to PAC, including PB and non-PB mechanisms. A previous Chinese study found that PB contributes to 38% of angle closure, and combined non-PB and PB mechanisms contribute to 54% of angle closure^[14]. Non-PB factors, which contribute to angle

crowding, include a thick peripheral iris, an anteriorly located peripheral iris, an anteriorly positioned CB, and a plateau iris. The degree of preoperative non-PB was negatively correlated with the peripheral anterior chamber widening after LPI. Anterior positioned CB is one of the most important non-PB mechanisms. Our results showed baseline CB position was predictive for angle changes after LPI. Multivariate regression showed that a qualitative anteriorly positioned CB was associated with reduced angle widening after LPI. The anterior position of the CB has been extensively proven to be a predisposing factor for angle closure, especially in Chinese patients^[24-25]. Anteriorly positioned CB occurred more frequently in closed angles than in opened angles after LPI in Chinese patients with PACS^[22]. In a study of 73 Korean PAC and PACG patients, using UBM and AS-OCT, Kwon *et al*^[26] found that a narrower TCA showed less effect on IOP lowering as an outcome of LPI.

In this study, we found that iris insertion was correlated with angle widening after LPI, suggesting that iris insertion is a predictive parameter for angle widening after LPI. LPI was associated with less angle widening in patients with a peripheral iris in closer proximity to the angle. It has been reported that eyes with basal iris insertion are prone to have angle closure than those without iris insertion^[27]. However, Yun *et al*^[28] found basal iris insertion did not affect angle widening after LPI based on AS-OCT images from nasal and temporal quadrants. Using UBM images from four quadrants, we found that iris insertion was marginally predictive and thus included in the predictive model.

Univariate linear regression analysis showed that a thinner iris thickness was correlated with greater angle widening. However, multivariate linear regression analysis did not identify iris thickness as an independent predictor for angle widening after LPI. Other non-PB factors, such as CB size and iris angulation, may contribute to angle closure PAC, but we did not find they were predictive for angle widening after LPI. As a key confounding factor, IC may affect other factors. Mizoguchi *et al*^[13] reported that lower baseline measurements of iris thickness are associated with greater iris curvature. Kwon *et al*^[26] reported that a flatter IC is associated with narrower TCA. Here, we categorized quadrants according to the configuration of IC to control the IC factor, and estimated the predictive factors for LPI outcome.

In the extreme IC group, which accounted for 30% of all quadrants, the mean AOD500 increased significantly by 220% (from 0.10 mm before LPI to 0.32 mm after LPI treatment). However, no predictive factor was found to be associated with angle widening in extreme IC quadrants. In the moderate IC quadrants, which accounted for approximately 70% of quadrants, the mean AOD500 increased by 55% (from 0.09 mm before

LPI to 0.14 mm after LPI treatment). Regression analysis showed that greater baseline iris angulation was correlated with less angle widening in the moderate IC group. The angle width remained unchanged in the absent IC quadrant group.

Plateau iris occurs in about 30% of Asian PACG eyes with a patent LPI^[29-30]. Iris angulation is one of key features for plateau iris configuration. It is speculated that plateau iris configuration occurred after LPI in the moderate IC group with iris angulation, a flatter IC, and a narrower TCA. In the present study, iris angulation was found to be the only significant predictor in the quadrants with moderate IC.

This study has some limitations such as the small sample size, especially in the AIC group. The inadequate sample size may reduce the power to identify significant differences between the groups. However, our analysis was mainly based on quadrants. The inclusion of four quadrants increased the sample size for data analysis. In addition, the classification of the qualitative assessment system was arbitrarily selected in this study. Difficulty in identifying some features may affect the classification results. Since pupil diameter can influence anterior segment parameter measurement due to light and fixation, pupil diameter was selected as a covariate for analysis. Finally, UBM images were not acquired in the dark. Anterior chamber angles are inclined to close in the dark; thus, dark UBM acquisition may improve our understanding of the mechanisms of angle closure.

In conclusion, the present study showed the effect of enlarging the anterior chamber angle and identified three predictive factors for greater enlargement of the anterior chamber angle, including IC, neutral positioned CB, and iris insertion at baseline. Quadrants with extreme IC exhibited substantial anterior chamber angle enlargement after LPI, but no predictive factors were identified. Quadrants with moderate IC showed mild angle widening after LPI, and iris angulation was found to be a predictor factor for a smaller change in the anterior chamber angle. Our findings show the angle-widening benefit of prophylactic LPI and may help guide treatment planning in PACS patients.

ACKNOWLEDGEMENTS

Conflicts of Interest: Pei XT, None; Wang SH, None; Sun X, None; Chen H, None; Wang BS, None; Li SN, None; Wang T, None.

REFERENCES

- 1 Tham YC, Li X, Wong TY, Quigley HA, Aung T, Cheng CY. Global prevalence of glaucoma and projections of glaucoma burden through 2040: a systematic review and meta-analysis. *Ophthalmology* 2014;121(11):2081-2090.
- 2 Chan EW, Li X, Tham YC, Liao JM, Wong TY, Aung T, Cheng CY. Glaucoma in Asia: regional prevalence variations and future projections. *Br J Ophthalmol* 2016;100(1):78-85.

- 3 Foster PJ, Buhrmann R, Quigley HA, Johnson GJ. The definition and classification of glaucoma in prevalence surveys. *Br J Ophthalmol* 2002;86(2):238-242.
- 4 Marchini G, Chemello F, Berzaghi D, Zampieri A. New findings in the diagnosis and treatment of primary angle-closure glaucoma. *Prog Brain Res* 2015;221:191-212.
- 5 Wang WJ, Song HF, Liu ZC. Computational study on the biomechanics of pupil block phenomenon. *Biomed Res Int* 2019;2019:4820167.
- 6 Sun XH, Dai Y, Chen YH, Yu DY, Cringle SJ, Chen JY, Kong XM, Wang XL, Jiang CH. Primary angle closure glaucoma: what we know and what we don't know. *Prog Retin Eye Res* 2017;57:26-45.
- 7 He MG, Jiang YZ, Huang SS, Chang DS, Munoz B, Aung T, Foster PJ, Friedman DS. Laser peripheral iridotomy for the prevention of angle closure: a single-centre, randomised controlled trial. *Lancet* 2019;393(10181):1609-1618.
- 8 Mou DP, Liang YB, Fan SJ, Peng Y, Wang NL, Thomas R. Progression rate to primary angle closure following laser peripheral iridotomy in primary angle-closure suspects: a randomised study. *Int J Ophthalmol* 2021;14(8):1179-1184.
- 9 Gupta R, Kumar R, Chauhan L. Anterior chamber morphology changes in eyes with narrow angles by Scheimpflug imaging: pilocarpine versus laser peripheral iridotomy. *Int Ophthalmol* 2021;41(6):2099-2108.
- 10 Chan PP, Tang FY, Leung DY, Lam TC, Baig N, Tham CC. Ten-year clinical outcomes of acute primary angle closure randomized to receive early phacoemulsification versus laser peripheral iridotomy. *J Glaucoma* 2021;30(4):332-339.
- 11 Qiu L, Yan YJ, Wu LL. Appositional angle closure and conversion of primary angle closure into glaucoma after laser peripheral iridotomy. *Br J Ophthalmol* 2020;104(3):386-391.
- 12 Chen SY, Wu LL. Effect of anatomic features of ciliary body on primary angle closure. *Zhonghua Yan Ke Za Zhi* 2018;54(9):716-720.
- 13 Mizoguchi T, Ozaki M, Wakiyama H, Ogino N. Peripheral iris thickness and association with iridotrabecular contact after laser peripheral iridotomy in patients with primary angle-closure and primary angle-closure glaucoma. *Clin Ophthalmol* 2014;8:517-522.
- 14 Wang N, Ouyang J, Zhou W, Lai M, Ye T, Zeng M, Chen J. Multiple patterns of angle closure mechanisms in primary angle closure glaucoma in Chinese. *Zhonghua Yan Ke Za Zhi* 2000;36(1):46-51,5,6.
- 15 Tanner L, Gazzard G, Nolan WP, Foster PJ. Has the EAGLE landed for the use of clear lens extraction in angle-closure glaucoma? And how should primary angle-closure suspects be treated? *Eye (Lond)* 2020;34(1):40-50.
- 16 Meduri E, Gillmann K, Bravetti GE, Niegowski LJ, Mermoud A, Weinreb RN, Mansouri K. Iridocorneal angle assessment after laser iridotomy with swept-source optical coherence tomography. *J Glaucoma* 2020;29(11):1030-1035.
- 17 Lee RY, Kasuga T, Cui QN, Huang GF, He MG, Lin SC. Association between baseline angle width and induced angle opening following prophylactic laser peripheral iridotomy. *Invest Ophthalmol Vis Sci* 2013;54(5):3763-3770.
- 18 Kirchhoff A, Stachs O, Guthoff R. Three-dimensional ultrasound findings of the posterior iris region. *Graefes Arch Clin Exp Ophthalmol* 2001;239(12):968-971.
- 19 Ma XY, Zhu D, Zou J, Zhang WJ, Cao YL. Comparison of ultrasound biomicroscopy and spectral-domain anterior segment optical coherence tomography in evaluation of anterior segment after laser peripheral iridotomy. *Int J Ophthalmol* 2016;9(3):417-423.
- 20 Moghimi S, Bijani F, Chen R, Yasseri M, He MG, Lin SC, Weinreb RN. Anterior segment dimensions following laser iridotomy in acute primary angle closure and fellow eyes. *Am J Ophthalmol* 2018;186:59-68.
- 21 Theinert C, Wiedemann P, Unterlauff JD. Laser peripheral iridotomy changes anterior chamber architecture. *Eur J Ophthalmol* 2017;27(1):49-54.
- 22 He MG, Friedman DS, Ge J, Huang WY, Jin CJ, Cai XY, Khaw PT, Foster PJ. Laser peripheral iridotomy in eyes with narrow drainage angles: ultrasound biomicroscopy outcomes. The Liwan Eye Study. *Ophthalmology* 2007;114(8):1513-1519.
- 23 Huang GF, Gonzalez E, Lee R, Osmonovic S, Leeungurasatien T, He MG, Lin SC. Anatomic predictors for anterior chamber angle opening after laser peripheral iridotomy in narrow angle eyes. *Curr Eye Res* 2012;37(7):575-582.
- 24 He N, Wu LL, Qi M, He MG, Lin S, Wang X, Yang F, Fan X. Comparison of ciliary body anatomy between American caucasians and ethnic Chinese using ultrasound biomicroscopy. *Curr Eye Res* 2016;41(4):485-491.
- 25 Henzan IM, Tomidokoro A, Uejo C, Sakai H, Sawaguchi S, Iwase A, Araie M. Comparison of ultrasound biomicroscopic configurations among primary angle closure, its suspects, and nonoccludable angles: the kumejima study. *Am J Ophthalmol* 2011;151(6):1065-1073.e1.
- 26 Kwon J, Sung KR, Han S, Moon YJ, Shin JW. Subclassification of primary angle closure using anterior segment optical coherence tomography and ultrasound biomicroscopic parameters. *Ophthalmology* 2017;124(7):1039-1047.
- 27 Ku JY, Nongpiur ME, Park J, Narayanaswamy AK, Perera SA, Tun TA, Kumar RS, Baskaran M, Aung T. Qualitative evaluation of the iris and ciliary body by ultrasound biomicroscopy in subjects with angle closure. *J Glaucoma* 2014;23(9):583-588.
- 28 Yun SC, Hong JW, Sung KR, Lee JY. Effects of laser peripheral iridotomy in subgroups of primary angle closure based on iris insertion. *J Ophthalmol* 2015;2015:581719.
- 29 Kumar RS, Tantisevi V, Wong MH, Laohapojanart K, Chansanti O, Quek DT, Koh VT, MohanRam LS, Lee KY, Rojanapongpun P, Aung T. Plateau iris in Asian subjects with primary angle closure glaucoma. *Arch Ophthalmol* 2009;127(10):1269-1272.
- 30 Nongpiur ME, Verma S, Tun TA, Wong TT, Perera SA, Aung T. Plateau iris and severity of primary angle closure glaucoma. *Am J Ophthalmol* 2020;220:1-8.